



THE UNIVERSITY *of* EDINBURGH

Edinburgh Research Explorer

Is the kinetoplast DNA a percolating network of linked rings at its critical point?

Citation for published version:

Michieletto, D, Marenduzzo, D & Orlandini, E 2015, 'Is the kinetoplast DNA a percolating network of linked rings at its critical point?', *Physical Biology*, vol. 12, no. 3, 036001. <https://doi.org/10.1088/1478-3975/12/3/036001>

Digital Object Identifier (DOI):

[10.1088/1478-3975/12/3/036001](https://doi.org/10.1088/1478-3975/12/3/036001)

Link:

[Link to publication record in Edinburgh Research Explorer](#)

Document Version:

Publisher's PDF, also known as Version of record

Published In:

Physical Biology

General rights

Copyright for the publications made accessible via the Edinburgh Research Explorer is retained by the author(s) and / or other copyright owners and it is a condition of accessing these publications that users recognise and abide by the legal requirements associated with these rights.

Take down policy

The University of Edinburgh has made every reasonable effort to ensure that Edinburgh Research Explorer content complies with UK legislation. If you believe that the public display of this file breaches copyright please contact openaccess@ed.ac.uk providing details, and we will remove access to the work immediately and investigate your claim.



Is the kinetoplast DNA a percolating network of linked rings at its critical point?

This content has been downloaded from IOPscience. Please scroll down to see the full text.

2015 Phys. Biol. 12 036001

(<http://iopscience.iop.org/1478-3975/12/3/036001>)

View [the table of contents for this issue](#), or go to the [journal homepage](#) for more

Download details:

IP Address: 129.215.72.120

This content was downloaded on 07/03/2016 at 15:06

Please note that [terms and conditions apply](#).

Physical Biology



PAPER

OPEN ACCESS

RECEIVED

20 March 2015

ACCEPTED FOR PUBLICATION

30 March 2015

PUBLISHED

13 May 2015

Content from this work may be used under the terms of the [Creative Commons Attribution 3.0 licence](#).

Any further distribution of this work must maintain attribution to the author(s) and the title of the work, journal citation and DOI.



Is the kinetoplast DNA a percolating network of linked rings at its critical point?

Davide Michieletto¹, Davide Marenduzzo² and Enzo Orlandini³¹ Department of Physics and Centre for Complexity Science, University of Warwick, Coventry CV4 7AL, UK² School of Physics and Astronomy, University of Edinburgh, Mayfield Road, Edinburgh EH9 3JZ, Scotland, UK³ Dipartimento di Fisica e Astronomia, Sezione INFN, Università di Padova, Via Marzolo 8, 35131 Padova, ItalyE-mail: d.michieletto@warwick.ac.uk**Keywords:** kinetoplast DNA, percolation, topology

Abstract

In this work we present a computational study of the kinetoplast genome, modelled as a large number of semiflexible unknotted loops, which are allowed to link with each other. As the DNA density increases, the system shows a percolation transition between a gas of unlinked rings and a network of linked loops which spans the whole system. Close to the percolation transition, we find that the mean valency of the network, i.e. the average number of loops which are linked to any one loop, is around three, as found experimentally for the kinetoplast DNA (kDNA). Even more importantly, by simulating the digestion of the network by a restriction enzyme, we show that the distribution of oligomers, i.e. structures formed by a few loops which remain linked after digestion, quantitatively matches experimental data obtained from gel electrophoresis, provided that the density is, once again, close to the percolation transition. With respect to previous work, our analysis builds on a reduced number of assumptions, yet can still fully explain the experimental data. Our findings suggest that the kDNA can be viewed as a network of linked loops positioned very close to the percolation transition, and we discuss the possible biological implications of this remarkable fact.

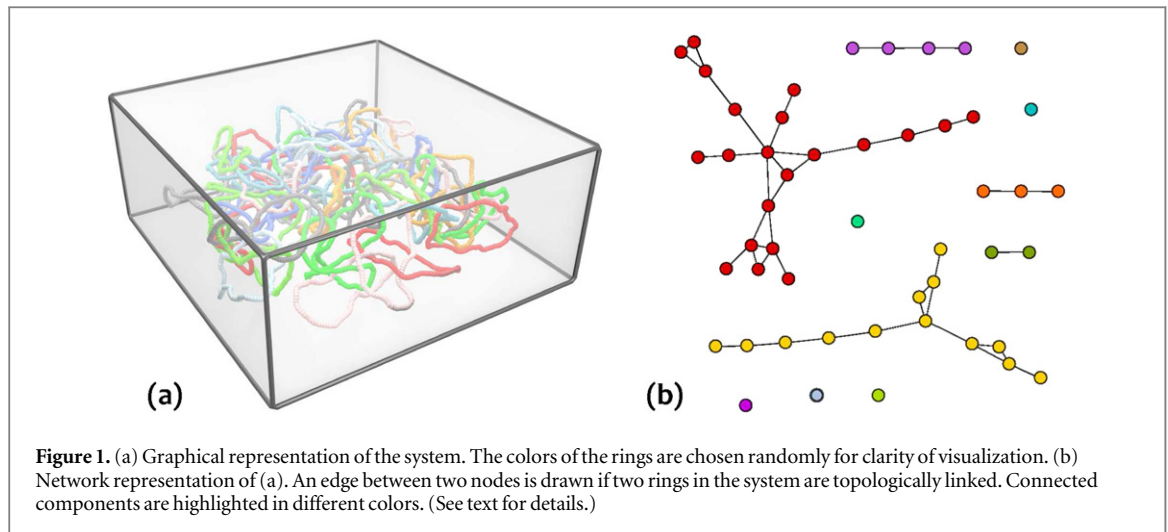
1. Introduction

A kinetoplast [1] is a network of linked DNA loops commonly found in a group of unicellular eukaryotic organisms of the class Kinetoplastida. Some of these organisms are responsible for important diseases such as sleeping sickness and leishmaniasis [2–4]. The kinetoplast DNA (kDNA) is known for its unique structure. Thousands of short (1–2.5 kbp) DNA loops are interlinked, forming a spanning network that fills the mitochondria. The short loops, or mini-circles, are also linked with few large circles, or maxi-circles, consisting of around 30–50 kbp [5]. The loops are found to be in a relaxed state, i.e. they are not supercoiled, contrarily to DNA loops in other similar organisms. *C. fasciculata* mini-circles assemble in a network whose shape resembles that of a disk which measures 1 μm in diameter and is 0.4 μm thick [6, 7]. Networks which are removed from the mitochondria, e.g. via cell lysis, expand into an elliptical shape whose minor and major axis are respectively around 10 μm and 15 μm , i.e. roughly a hundred times bigger than

their dimension *in vivo* [7]. This suggests that the networks experience a confinement within the mitochondria.

It has been observed [8] that a ‘tripartite attachment complex’ keeps the kinetoplast statically in place near the basal body, from which it is physically separated by the mitochondrial envelope. Transmission electron microscopy images of kinetoplast networks *in vivo* [8–12] also suggest that the shape of the mitochondrial membrane near the kinetoplast acts as a physical constraint on the outer structure of the network, while it is likely that histone-like proteins, such as p16, p17 and p18, or ‘KAP proteins’ encoded in genes KAP2, KAP3 and KAP4, act as chemical constraint on the inner structure [13–16].

The concentration of DNA in the kinetoplast has been found to be around 50 mg ml^{-1} [5], similar to that found in bacteria (20 mg ml^{-1}) but far smaller than the one inside the head of a T4 bacteriophage (800 mg ml^{-1} or more) [17], meaning that the loops are overlapping but there is considerable space between DNA strands [5].



Previous findings strongly suggest that the loops in the network are linked once with their neighbours, and that the valence of each rings, i.e. the number of neighbours, is around 3. In other organisms of the same class, e.g. *L. tarentolae*, the valence number is smaller, probably due to their different DNA concentration. During replication, catenation between the loops introduces a nontrivial topological problem, which is solved as follows. First topoisomerase II disentangles one loop at a time from the network, the loop then undergoes duplication in a complex nearby, and later on it links again to the periphery of the network, together with the progeny mini-circles [6, 18]. At this stage, each circle has a valence which is higher than 3: again, most likely due to the increase in density following DNA synthesis [19]. Finally, when the cell divides, two copies of the network are produced and the valence number is brought back to 3. This change in network valence has to be mediated by topological enzymes, e.g. topoisomerases, also accompanied by a relaxation of mass (mini-circle) density.

The topology of the kDNA network is unique in its own kind and has been studied in the past with experiments and simplified models [20, 21], but a full understanding of its role, origin and replication continues to represent a challenge for the scientific community [9, 22, 23].

Here we propose a model which builds on fewer assumptions with respect to previous work in the literature. Phantom semi-flexible rings are confined to move inside a box of linear size L , which we vary in order to simulate varying values of the density of the kinetoplast network inside the mitochondrial membrane. By computing the Gauss linking number between pairs of rings, we analyse the topological constraints experienced by the rings within the system. The model kDNA can be naturally represented as a network, by mapping rings to nodes and links between two rings to (undirected) edges [24, 25] (see figure 1). Our findings suggest that for densities ρ greater than a critical density ρ_p , the system has a non-zero

probability of forming a cluster of linked rings as big as the size of the whole system, i.e. percolating. In the case of the kinetoplast, a network with this property can be viewed as a state in which a relevant fraction of the mini-circles in the kinetoplast are mutually interlocked to form an extended collection of inseparable rings [21]. We also further study the topology of the network by simulating its digestion, which is realized experimentally, for instance, by adding nuclease or restriction enzymes that cut the DNA, to the solution containing the mini-circles. Remarkably, the simulated digestion provides results which are quantitatively comparable with experiments [25], and give new insight into the origin of the network.

2. Model

We model the kinetoplast genome as $N = 50$ DNA rings, each of which is a worm-like polymer made of $M = 128$ beads of size σ and with persistence length $l_p = 20 \sigma$. A cut-and-shift form of the Lennard-Jones potential is used to model steric interaction between beads belonging to the same chain, so that we ensure that the rings do not get knotted and that they assume self-avoiding configurations. In physical units, $\sigma \simeq 2.5$ nm is the hydrated diameter of double-stranded DNA, $l_p \simeq 50$ nm, while the contour length of each of the loops is $L_c = 128 \sigma = 320$ nm $\simeq 1$ kbp. The network is enclosed in a box of size $L_1 \times L_1 \times L_2$, with L_i between 200 and 80 (in units of σ). The boxes considered are both symmetric, i.e. $L_1 = L_2$, and asymmetric, i.e. $L_1 = 2L_2$, such as the aspect ratio is similar to that of a kinetoplast disk, whose thickness *in vivo* (0.4 μ m) is roughly half of its diameter (1 μ m).

We sample different network configurations by letting the rings thermalise with no steric interaction between different rings (i.e. rings are invisible to each other during equilibration), for at least the time taken for a ring to diffuse its own gyration radius, i.e. $\tau_R = R_g^2/D_{CM}$. This stage mimics the presence of

topological enzymes such as topoisomerases, which can either link or un-link the mini-circles from the neighbours. This allows the mini-circles to freely diffuse while temporarily unlinked. After this interval, we turn a soft repulsion on, which acts on every pair of beads distant r to each other and which we model as:

$$E_s(r) = A(0, 50; 10^5) \left(1 + \cos \left(\frac{\pi r}{r_c} \right) \right),$$

with $A(x, y; t)$ a ramp function which brings $A(x, y; t)$ from x to y in t timesteps and $r_c = 2^{1/6}\sigma$. After this operation, which ensures that no contours are overlapping, we compute the pairwise Gauss linking number of any two rings, defined as:

$$Lk(i, j) = \frac{1}{4\pi} \int_{\gamma_i} \int_{\gamma_j} \frac{|\mathbf{r}_i - \mathbf{r}_j|}{|\mathbf{r}_i - \mathbf{r}_j|^3} \cdot (d\mathbf{r}_i \times d\mathbf{r}_j), \quad (1)$$

where γ_i and γ_j are the contours of the two rings, and \mathbf{r}_i and \mathbf{r}_j the respective spatial coordinates [26, 27]. This is a topological invariant which describes the pairwise state of rings, as far as we forbid two rings to pass through each other. This stage represents the final kinetoplast conformation, when no molecule of topoisomerase is available. Once the linking number has been measured, we turn the soft potential off and repeat the procedure in order to obtain an ensemble of (independent) configurations for a given density ρ .

It is important to bear in mind that this ensemble of networks should be interpreted as a collection of independent equilibrated networks, rather than as a dynamical sequence of network conformations over time, since in reality the mini-circles are not allowed to cross through each other without the intervention of a topological enzyme. In other words we are generating ensembles of networks that one could obtain, for instance, when looking at the kinetoplast after replication and after it has been separated into the two daughter cells. At this stage in fact, a simultaneous topological and structural re-arrangement of the network has to take place, involving both, topological enzymes and mass relaxation via mini-circles diffusion, which is itself allowed by the presence of topoisomerases.

The model we propose here is, with respect to previous work, based on less assumptions, as, for example, it does not rely on the fact that the mini-circles are anchored on a 2D lattice [21]. This is an important assumption that we relax. In fact, this rigid structure would severely compromise the kinetoplast replication, hindering the free removal of mini-circles. We will here show that the 2D layer structure of the kinetoplast, which is widely reported in the literature, is not required to obtain agreement with experimental observations. This suggests that condensation and anchoring into a layered 2D structure is secondary to the network topological arrangement. Furthermore, we here relax the assumption that the rings are perfect

circles [20], and consider much more realistic semi-flexible polymers.

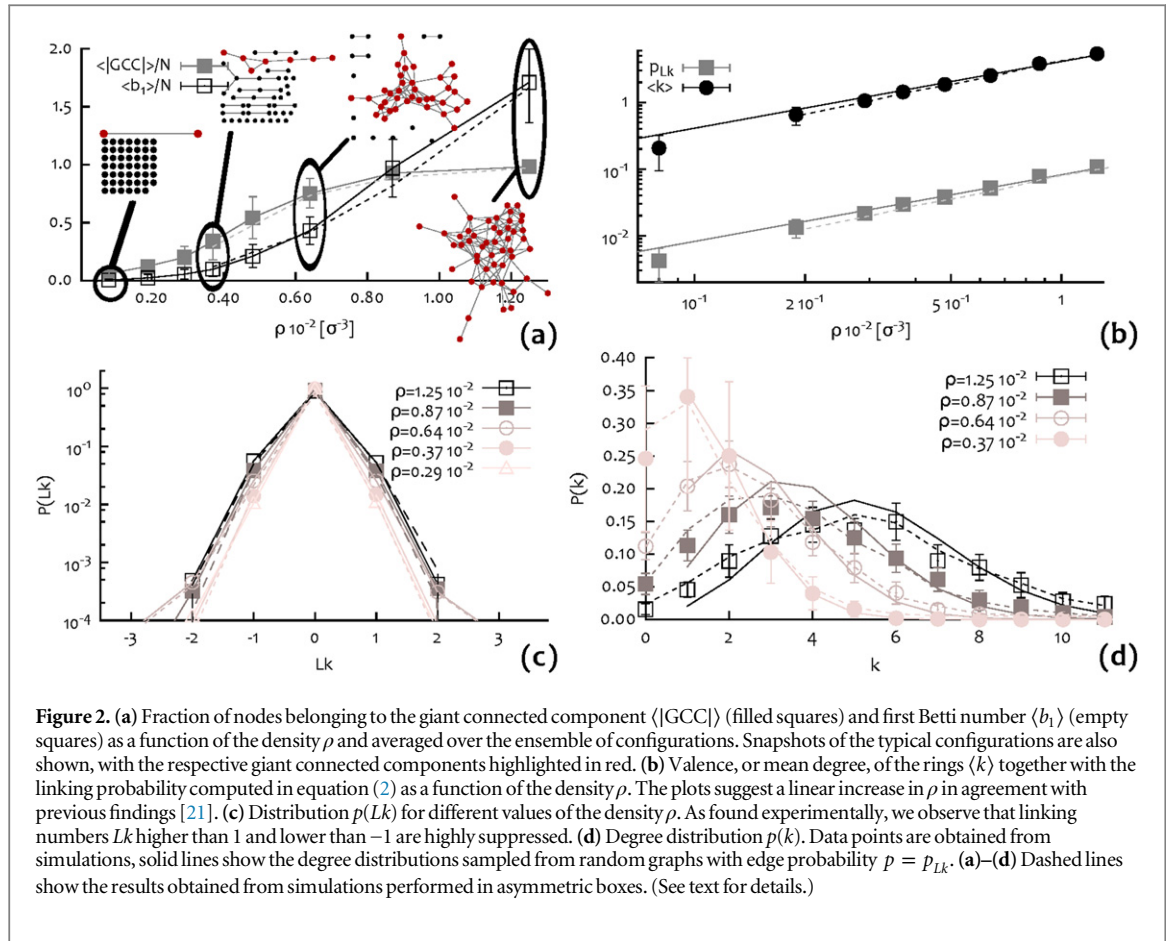
The observables we measure from these networks are averaged over the ensemble formed by 5000 configurations generated with the method described above. For each configuration in the ensemble, we generate a corresponding network representation by assigning an (undirected) edge between each two rings which have $Lk(i, j) \neq 0$ [24, 25]. This maps the system of linked rings to an undirected network, whose properties are directly related to the properties of the system of linked rings (see figure 1). Note that, because this procedure is based on the pairwise linking number, it would classify Borromean and Brunnian links as unlinked; we expect such non-trivial links to be rare within the kinetoplast network, where a good approximation is that each mini-circle is linked identically and once to its neighbours [7, 25].

Our main control parameter is the size of the confining container, L_b , which we modify to vary the density ρ . This determines the physical properties of the resulting network. The overlapping (number) density ρ^* , at which rings start to feel each other, can be estimated as $\rho^* = M/(4/3\pi R_g^3) \sim 0.0076\sigma^{-3}$, where R_g has been measured from relaxed rings in sparse solution¹. To convert to a biologically realistic value, we may assume that the volume occupied by each bead is that of a cylinder of size and height equal to σ , which leads to a volume fraction $\phi^* \sim 0.60\%$ occupied by the DNA, or equivalently a concentration $c^* \sim 8.1 \text{ mg ml}^{-1}$ (calculated with a DNA density $\rho_{\text{DNA}} = 1.35 \text{ g cm}^{-3}$ [28]).

3. Results

A good way of studying the properties of a network G is by looking at its first Betti number $b_1(G)$ and its giant connected component $\text{GCC}(G)$ [24]. The former is defined as $b_1(G) \equiv N_{\text{CC}} - |\mathcal{V}| + |\mathcal{E}|$, where N_{CC} is the number of connected components and $|\mathcal{V}|$ and $|\mathcal{E}|$ the size of the sets of vertices and edges, respectively. The latter is defined as the largest set of nodes in which every node can be reached by any other node within the set. For instance, in figure 1, the GCC corresponds to the red cluster. This quantity is useful to investigate the ‘percolation’ of the network. Here we define a network to be percolating if the size of the GCC is of the same order as the number of nodes in the whole network. The percolation density ρ_p is then the density above which the system shows a non-zero probability of percolation. The GCC of a percolating network is a spanning, or percolating, cluster. While the size of the GCC gives some information regarding the connectivity of the network, the first Betti number,

¹ We find $R_g \sim 16\sigma$, close to but below the estimate $R_g \sim \sqrt{L_c l_p/6} \sim 20.7\sigma$ which works for $L_c \gg l_p$ and disregards excluded volume interactions within one ring.



$b_1(G)$, provides us with some insight about the topology of the network. In fact, $b_1(G)$ equals the number of closed sub-graphs in the network, which is also the total number of cyclic d-mers [24]. For mostly unconnected graphs, $b_1(G) \simeq 0$, while for nearly fully connected graphs: $|\mathcal{E}| \simeq N(N-1)/2$ and hence $b_1(G) \simeq N^2/2$ for large N . An increase in $b_1(G)$ corresponds to both, an increase in network connectivity and an increase in cyclic structures.

In figure 2(a) we show the size of the GCC, and the first Betti number of the graph G , $b_1(G)$, divided by the size of the system N as a function of the system density ρ . This plot suggests that a percolating component can be observed in the system at values of the density $\rho \gtrsim \rho_p \simeq 0.0064 \sigma^{-3}$. Although the precise value of the percolation density is not well defined for finite systems, our model allows to predict the emergence of a state in which a fraction close to unity of rings in the system is topologically interlocked in a single cluster for values of the density above ρ_p . In figure 2(b) the valence, or mean vertex degree $\langle k \rangle$ is shown together with the linking probability p_{Lk} as a function of the density ρ . The figure shows that the average degree $\langle k \rangle$ scales linearly with the density ρ , in agreement with previous findings [21]. One can also see that at $\rho = \rho_p$ the valence of our network is three, in agreement with experiments [25]. By assuming that the network configurations are sampled from an ensemble of random

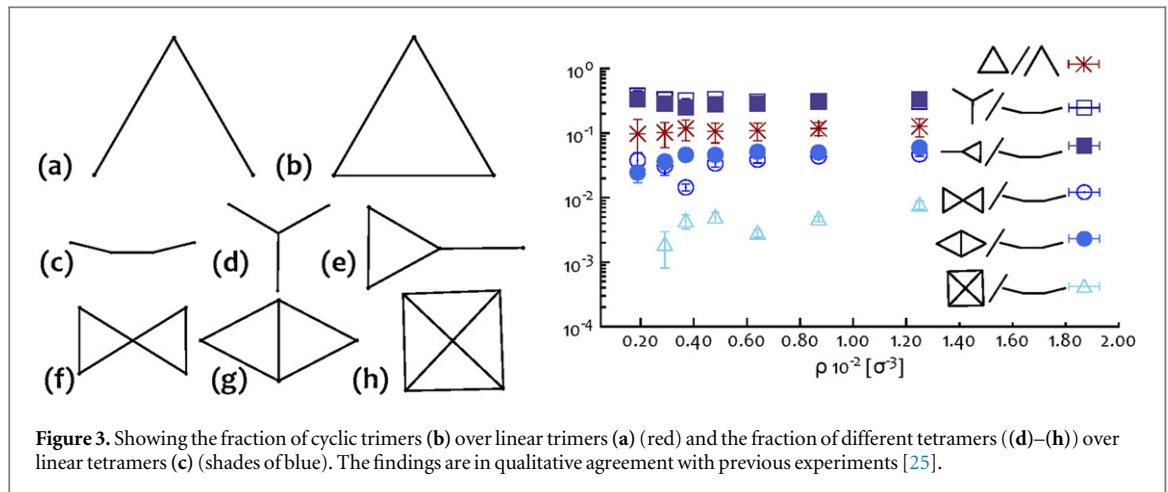
graphs, the linking probability p_{Lk} can be calculated as

$$p_{Lk} = \langle k \rangle / (N - 1). \quad (2)$$

The assumption that the network configurations can be described by random graphs is not justified *a priori*. On the other hand, we can check that this assumption is valid by comparing the degree distribution $p(k)$ obtained from the simulations (see data points and dashed lines in figure 2(d)) and the random graph distributions $p_{rg}(k; p)$ with $p = p_{Lk}$ obtained from equation (2):

$$p_{rg}(k; p_{Lk}) = \binom{N-1}{k} p_{Lk}^k (1 - p_{Lk})^{N-1-k}.$$

One can notice that the random graphs distributions and the data points are in very good agreement for $\rho \lesssim 0.0064 \sigma^{-3}$ and in agreement, but not as good, for $\rho \gtrsim 0.0087 \sigma^{-3}$; in other words, the system can be approximated as a random graph with linking probability p_{Lk} which is directly proportional to the valence of the rings and inversely proportional to the number of rings in the box. In terms of the kinetoplast structure one can imagine that, due to the presence of topological enzymes, the mini-circles can be un-linked and hence undergo free diffusion inside the mitochondrion. Because of this, it is reasonable to expect that the network of mini-circles would form a random arrangement of linked rings. In this respect, our model can capture the randomness of the system in a better



way than previous models found in the literature could.

In figure 2(c) we show the distribution of the linking number $p(Lk)$. This quantity is found to be peaked at zero for any density ρ investigated in this work. This means that the networks produced by our model are never fully connected, i.e. there are always more pairs of rings which are unlinked than pairs which are linked. The ‘shoulders’ of the distribution at $Lk = \pm 1$ increase with ρ although values of $|Lk| > 1$ are very unlikely ($p(Lk) < 10^{-3}$). This is once again in agreement with experimental findings [7, 25], which observed that each linked mini-circle is linked only once with its neighbours. For simplicity, we always assign a single edge between a pair of nodes even in those cases in which they have an higher linking number. Because they are so rare, they represents a small fraction of all the links, which can be neglected. The mean linking number $\langle Lk \rangle$ is zero within errors, as must be the case as configurations with $Lk = -1$ are as likely as ones with $Lk = +1$.

It is worth noting that in figures 2(a)–(d) we report the results obtained by simulating the system in asymmetric boxes. These are shown as dashed lines. As one can notice, the two cases are in very good qualitative agreement. Small deviations are found for the degree distributions and the average Betti number $\langle b_1 \rangle$. This suggests that the actual shape of the confining box does not affect the qualitative behaviour of the system, which preserves its randomness.

In figure 3(a)–(h) we show all the possible sub-graphs with three and four nodes, up to symmetries. We call these patterns ‘motifs’. Every connected graph formed by three and four nodes is isomorphic to those in figures 3(a) and (b) and 1(c)–(h), respectively. In order to count the number of motifs of each type, we consider every connected sub-graph with given number of nodes and check whether it is isomorphic to one of the motifs shown in figure 1. The results are shown in figure 3. We observe that linear trimers (motif 3(a)) are much more frequent than cyclic ones (motif 3(b)), for any density ρ . Similarly, linear

tetramers, are three times more common than branched tetramers (motif 3(d)), which is in qualitative agreement with experiments [25]. Finally, fully cyclic tetramers are highly suppressed, again in agreement with previous experimental work.

To further quantitatively compare the properties and structure of the random network of linked confined loops found in simulations to those of the kDNA, and inspired by the common biological procedure known as ‘digestion’, we simulate the presence in solution of restriction enzymes, i.e. enzymes which are able to cut DNA strands. In this way we can simulate the random breakage of the network due to a concentration of restriction enzymes which can cut the network, and which was used in [25] to further study the network topology experimentally. To model digestion *in silico*, we associate a probability p to each bead composing the rings to be removed. Such probability is related to the concentration of restriction enzymes in the solution and time left to act on DNA mini-circles. The equivalent probability p_r of a ring to become linearized, e.g. by removing one or more of its beads, is

$$p_r = 1 - (1 - p)^M \sim Mp, \quad (3)$$

where M is the number of beads composing the rings. For probability $p = p_r = 1/M$, every ring has been cut, on average, once, and therefore there are no longer closed rings in the system. This procedure maps to the network representation as we can assign the same probability p_r to each of the nodes, and with probability p_r we remove a node from the network. In practice, we consider an ensemble of (independent) configurations from the molecular dynamics simulation and for each one we simulate ten digestions by removing nodes at random with probability p_r from the corresponding network. We then average the observables over the ensemble of 50×10^3 simulated digestions. The average number of removed nodes is $\langle n_r \rangle = p_r N$. At the end of the (partial) digestions we measure the fraction of monomers (single uncate-nated rings), dimers (two catenated rings) and trimers (three catenated rings) obtained from the digested network. These quantities can be obtained by running

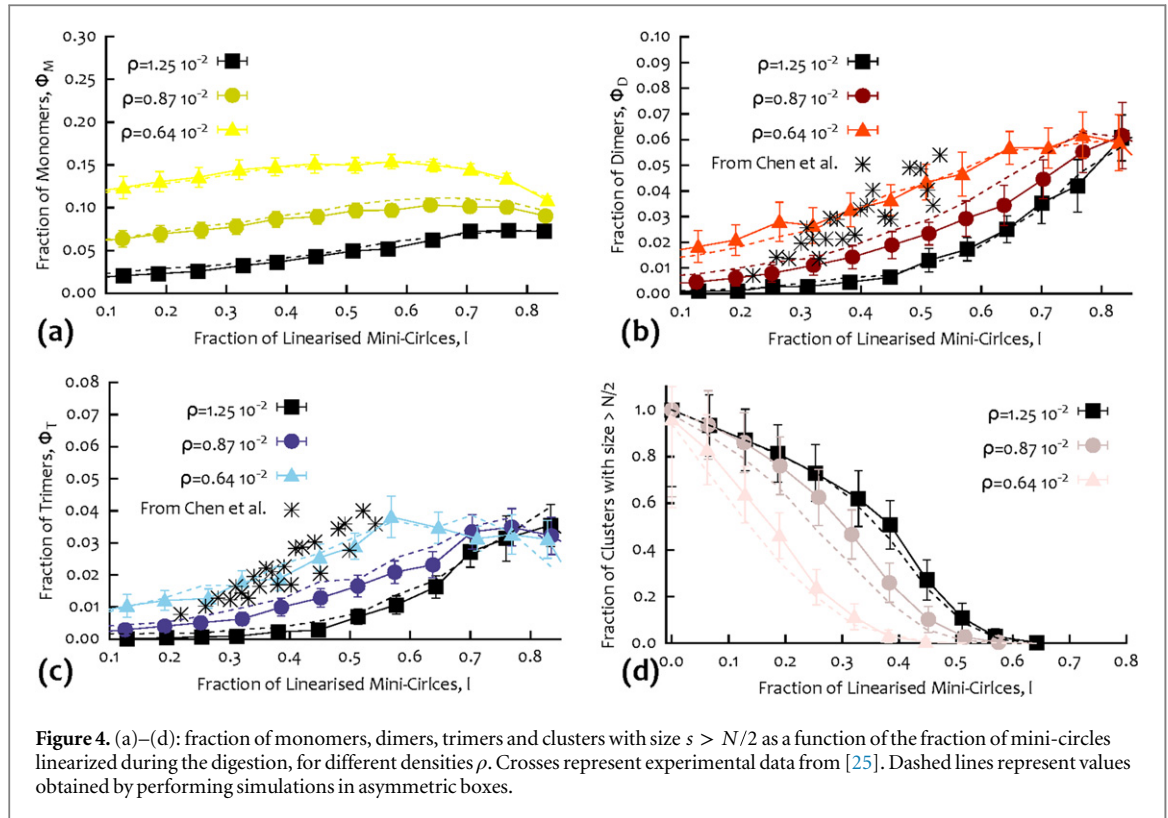


Figure 4. (a)–(d): fraction of monomers, dimers, trimers and clusters with size $s > N/2$ as a function of the fraction of mini-circles linearized during the digestion, for different densities ρ . Crosses represent experimental data from [25]. Dashed lines represent values obtained by performing simulations in asymmetric boxes.

a high resolution gel electrophoresis test on the samples, as in [25]. The relative fraction of monomers, dimers, trimers etc, correlates directly with the intensity of the bands, as these oligomers move with different speed in the gel. In figure 4 we report our findings for different values of density ρ , as a function of the linearized fraction of mini-circles, $l = \langle n_r \rangle$ (to ease comparison with the data in [25]).

From the results in figure 4(d), one can notice that even after half of the nodes have been removed, one can still observe some large, or percolating, clusters. In other words, the network shows high resistance against random breakage. When viewed as a property of the biological kinetoplast genome, this appears to be functionally relevant: the DNA network needs to remain intact either when some of the mini-circles are removed, e.g. by topoisomerase II, either accidentally during the cell cycle, or during replication when decatenation is required.

The distribution of the fraction of monomers Φ_M , dimers Φ_D and trimers Φ_T show peaks as a function of l , whose locations depend on the density. In general, the value of ρ at which the distributions reach their maximum increases with density, meaning that the denser the system, the more it has to be digested before the probability of observing monomers, dimers or trimers, rises and becomes sizeable. For fixed density, the peaks show that trimers are best produced at lower l than dimers, and dimers at lower l than monomers; this is expected as increasing l should increase the probability of finding smaller and smaller catenanes.

We find that the best range of l within which gel electrophoresis of oligomers can give information on the network structure depends on the density ρ . For the highest density studied here, the fraction of linearized mini-circles has to be close to 80%, while for $\rho \sim 0.0064 \sigma^{-3}$ the value of l can lay between 30% and 80%, after which the survival fraction of dimers and trimers start to decrease. This range is very similar to the one observed in [25]. Even more strikingly, in figure 4 we superimpose the data from [25], and observe a striking quantitative agreement with the curve for $\rho = 0.0064 \sigma^{-3}$ —we recall that $\rho = 0.0064 \sigma^{-3}$ also leads to $\langle k \rangle \simeq 3$ as inferred from the experiments. Remarkably, considering the asymmetric system results in very little difference with the curves reported in figure 4. This strongly suggests that the simple symmetric confinement is enough to understand the kinetoplast structure both qualitatively and quantitatively.

The good agreement with experimental data shown in figure 4, strongly suggests that our model can capture the topological structure of the kDNA described by a network of randomly connected confined 3D links close to the percolation transition. In this respect, the fact that the kDNA is found geometrically to be a layered disk-shaped structure may be due to a combination of the geometrical spatial confinement the network is subject to *in vivo* [8–12, 21] and of the action of histone-like DNA-binding proteins [13–16]. However, the latter is inessential to explain the existing digestion data. In addition, in the

supplementary material we show that this layered organized structure can be achieved within our framework by adding suitable interactions between some parts of the rings and the confining box (see S.I. for details).

One of the main conclusions that can be drawn from our work is that the kinetoplast topology is independent on the network packaging and organization, while it is driven solely by geometrical confinement. This prediction can be tested, for instance, by measuring the valence of *in vivo* networks, as done in [19, 25], formed when genes expressing KAP histone-like proteins are silenced, as done in [16]. Our results predict that in this case, the kinetoplast should appear unlayered and disorganized, while retaining a valence near 3.

4. Discussion and conclusions

In summary, we studied the statistical physics of a percolating cluster of linked rings, by confining phantom semiflexible rings in a box and varying the density. The onset of the percolation occurs at concentrations $\rho_p \sim 0.0064 \sigma^{-3}$. At this density, the mean valence of the nodes is around three, which is compatible with the findings in the kDNA. Importantly, at the same density value, we compared the results from an *in silico* digestion of the network by a restriction enzyme, finding very good quantitative agreement with the experimental data found in [25]. These results strongly suggest that the kinetoplast topology is well represented by this model at density $\rho \sim \rho_p$, i.e. by a network of linked rings close to its critical point, i.e. the point at which the network starts to show percolating behaviour. Remarkably, our results are affected very little by the details of the confining geometry—what matters is the presence of confinement itself, which drives the percolation transition in the network of links [21].

Our findings also suggest that the density of DNA loops in the kinetoplast networks should not be too far from the overlap density. Taking a typical case with $N = 5000$ loops of say 1 kbp each, we find that the overlap density is $\sim 8.1 \text{ mg ml}^{-1}$; the density of the same network within a mitochondrion of volume $\sim 1 \mu\text{m}^3$ volume is about 5.43 mg ml^{-1} , which fits very well with our simulations. The DNA structure in *C. fasciculata*, which is well studied, has larger density ($\sim 50 \text{ mg ml}^{-1}$), but this is achieved by further compaction by histone-like proteins [15, 16], hence does not reflect purely geometric confinement. Furthermore, even if the density is larger than the overlap density, a network could still exist close to the percolation transition if the activity of topoisomerase II, which allows catenation and is tacitly assumed by our model as loops are invisible to each other, is limited, for instance by the enzymatic concentration.

Being close to the percolation transition may well provide an evolutionary advantage for the kDNA network, as this structure may be favoured over a more heavily connected network, as it facilitates the decatenation during replication, but at the same time ensures that mini-circles are not released by mistake. Another property of the kinetoplast-like network is that it is very resistant to digestion by a restriction enzyme, i.e. the digestion has to proceed significantly before large clusters disappear (see figure 4). This feature again appears to be functionally relevant, as it provides a way to preserve genetic material against random breakage and replication mistakes.

Acknowledgments

DMi acknowledges the support from the Complexity Science Doctoral Training Centre at the University of Warwick with funding provided by the EPSRC (EP/E501311). EO acknowledge financial support from the Italian ministry of education grant PRIN 2010HXAW77. We also acknowledge the support of EPSRC to DMA, EP/I034661/1. The computing facilities were provided by the Centre for Scientific Computing of the University of Warwick with support from the Science Research Investment Fund.

References

- [1] Fairlamb A H, Weislogel P O, Hoeijmakers J H and Borst P 1978 *J. Cell Biol.* **76** 293–309
- [2] Young D and Morales A 1987 *J. Med. Entomol.* **24** 587–9
- [3] Jacobson R L 2003 *Folia parasitol.* **50** 241–50
- [4] MacLean L, Chisi J and Odiit M 2004 *Infect. Immun.* **72** 7040–4
- [5] Shapiro T and Englund P 1995 *Annu. Rev. Microbiol.* **49** 117–43
- [6] Pérez-Morga D L and Englund P T 1993 *Cell* **74** 703–11
- [7] Jensen R E and Englund P T 2012 *Annu. Rev. Microbiol.* **66** 473–91
- [8] Ogbadoyi E, Robinson D and Gull K 2003 *Mol. Biol. Cell* **14** 1769–79
- [9] Lukeš J, Guilbride D and Votýpka J 2002 *Eukaryotic Cell* **1** 495–502
- [10] Gluenz E, Shaw M K and Gull K 2007 *Mol. Microbiol.* **64** 1529–39
- [11] Lai D h, Hashimi H, Lun Z r, Ayala F J and Lukes J 2008 *Proc. Natl Acad. Sci. USA* **105** 1999–2004
- [12] Docampo R, Ulrich P, Moreno S N J, Docampo R, Ulrich P and Moreno S N J 2010 *Phil. Trans. R. Soc. B* **365** 775–84
- [13] Xu C and Ray D S 1993 *Proc. Natl Acad. Sci. USA* **90** 1786–9
- [14] Xu C W, Hines J C, Engel M L, Russell D G and Ray D S 1996 *Mol. Cell. Biol.* **16** 564–76
- [15] Hines J C and Ray D S 1998 *Mol. Biochem. Parasitol.* **94** 41–52
- [16] Avliyakov N K, Lukes J and Ray D S 2004 *Eukaryot. Cell* **3** 518–26
- [17] Kellenberger E, Carlemalm E, Sechaud J, Ryter A and Haller G 1986 *Bacterial Chromatin* ed C O Gualerzi and C L Pon pp 11–25 (Berlin: Springer)
- [18] Liu B, Liu Y, Motyka S A, Agbo E E C and Englund P T 2005 *Trends Parasitol.* **21** 363–9
- [19] Chen J, Englund P T and Cazzarelli N R 1995 *EMBO J.* **14** 6339–47
- [20] Arsuaga J, Blackstone T, Diao Y, Karadayi E and Saito M 2007 *J. Phys. A: Math. Theor.* **40** 1925–36

- [21] Diao Y, Hinson K, Kaplan R, Vazquez M and Arsuaga J 2012 *J. Math. Biol.* **64** 1087–108
- [22] Silver L E, Torri A F and Hajduk S L 1986 *Cell* **47** 537–43
- [23] Morris J C, Drew M E, Klingbeil M M, Motyka S A, Saxowsky T T, Wang Z and Englund P T 2001 *Int. J. Parasitol.* **31** 453–8
- [24] Michieletto D, Marenduzzo D, Orlandini E, Alexander G P and Turner M S 2014 *ACS Macro Lett.* **3** 255–9
- [25] Chen J, Rauch C A, White J H, Englund P T and Cozzarelli N R 1995 *Cell* **80** 61–69
- [26] Orlandini E, Tesi M C and Whittington S G 2000 *J. Phys. A: Math. Gen.* **33** 181–6
- [27] Orlandini E and Whittington S G 2004 *J. Chem. Phys.* **121** 12094–9
- [28] Matthews B 1968 *J. Mol. Biol.* **33** 491–7